Gradient algorithm for Hamiltonian identification of open quantum systems

Shibei Xue,[1,2,*] Rebing Wu,[3] Shan Ma,[4] Dewei Li,[1,2] and Min Jiang[2,5]

[1]*Department of Automation, Shanghai Jiao Tong University, Shanghai 200240, People's Republic of China*

[2]*Key Laboratory of System Control and Information Processing, Ministry of Education of China, Shanghai 200240, People's Republic of China*

[3]*Department of Automation, Tsinghua University, Beijing 100084, People's Republic of China*

[4]*School of Automation, Central South University, Changsha 410083, China and Peng Cheng Laboratory, Shenzhen 518000, People's Republic of China*

[5]*School of Electronics and Information Engineering, Soochow University, Suzhou 215006, People's Republic of China*

(Received 22 October 2020; accepted 24 December 2020; published 10 February 2021)

In this paper, we present a gradient algorithm for identifying unknown parameters in an open quantum system from the measurements of time traces of local observables. The open system dynamics is described by a general Markovian master equation based on which the Hamiltonian identification problem can be formulated as minimizing the distance between the real time traces of the observables and those predicted by the master equation. The unknown parameters can then be learned with a gradient descent algorithm from the measurement data. We verify the effectiveness of our algorithm in a circuit QED system described by a Jaynes-Cummings model whose Hamiltonian identification has been rarely considered. We also show that our gradient algorithm can learn the spectrum of a non-Markovian environment based on an augmented system model.

DOI: 10.1103/PhysRevA.103.022604

I. INTRODUCTION

Quantum information technology has attracted much attention in the past decades, including physically absolutely secure quantum communication and a huge acceleration in quantum computation [1]. These advantages rely on high-precision quantum operations designed with good models of the quantum information carriers, e.g., superconducting qubits or quantum dots, etc. However, it would not be easy to obtain a complete model for a quantum system. For example, in a recent experiment on a quantum dot system, the calculation based on a Markovian system model without containing the exact effect of noises arising in the environment fails to match the experimental data [2]. In addition, the inaccuracy of parameters in a model of quantum systems would also lead to errors in quantum computation.

Quantum identification is the crucial step towards obtaining a complete and accurate model, which utilizes the data of excitations and measurements to extract unknown information. In particular, Hamiltonian identification has gradually become a hot topic, whose task is to estimate unknown parameters in the Hamiltonian or to identify unknown structures in a quantum system. For closed quantum systems, an inversion-algorithm-based learning approach was presented to identify both the free Hamiltonian and the dipole for a class of molecular systems [3]. Employing the system's algebraic properties, the identification algorithms were proposed for special finite-level quantum systems, such as two-level systems [4,5], spin-1 systems [6], and spin networks [7], which can largely save the resources for the identification by measuring a smaller number of observables [8,9] or without state initialization [10]. For example, only one local observable is required for Hamiltonian identification of a three-spin-chain system [11]. Also, it is important that entangled observables were found to be more efficient than product observables in Hamiltonian identification [12]. Moreover, several systematic approaches were also explored for Hamiltonian identification. In Refs. [13,14], a quantum observer was designed for estimating the unknown parameters of a qubit, which is driven by the measurement results. Similarly, a Bayesian estimation method was presented for a two-qubit system, which can fulfill the Hamiltonian identification under noisy measurement data [15]. In addition, quantum process tomography [16] and quantum state tomography [17] approaches were generalized to the Hamiltonian identification, which rely on the accurate estimation of the evolutions or the states in the time-consuming tomography process. Besides the above time-domain approaches, a class of transfer-function-based frequency-domain approaches was presented for spin networks [18], where the unknown parameters can be obtained by solving a set of nonlinear algebraic equations induced by a measurement-result-induced realization. This method was experimentally realized in a nuclear magnetic resonance system [19]. However, the performance of the above methods would degrade when they are applied to real quantum systems which are open in general, i.e., coupled to a thermal bath or other quantum systems resulting in their dissipative dynamics.

For the identification of open quantum systems, several quantum identification methods were presented. The transfer-function-based method in Ref. [18] was extended to Markovian quantum systems [20], i.e., the quantum system in a memoryless environment with a short correlation time. A similar work can also be found in Ref. [21]. Moreover,

*shbxue@sjtu.edu.cn

a maximum-likelihood estimation method was proposed for an atomic maser system where the detection process can be considered a discrete-time Markovian chain [22,23]. Alternatively, continuous measurements can be applied for the Hamiltonian identification of finite-level open quantum systems [24–26]. Moreover, classical identification methods were extended to linear quantum systems such as quantum harmonic-oscillator networks [27,28]. However, when the quantum system involves interacting both finite-level and infinite-level subsystems, which is common in cavity QED systems, the underlying complicated algebra and nonlinear dynamics make the identification much harder. To our knowledge, such problems have not been explored in the literature.

In this paper, we propose a gradient algorithm for the identification of such quantum systems. To this aim, we describe the open quantum system by a general Markovian master equation, and the time traces of a selected set of observables are used for identifying the Hamiltonian such that the state of the system at a time instant can be expressed in terms of a series of evolution superoperators acting on the initial state of the system. We verify the effectiveness of our algorithm with a Markovian Jaynes-Cummings model in cavity (circuit) or quantum electrodynamical systems [29,30]. The performance of our algorithm under low-sampled data and noisy measurements is also tested in this system. In addition, we apply our algorithm to learn the spectrum of a non-Markovian environment associated with a colored quantum noise with a long correlation time [31,32]. In the literature, a differential algorithm [33], a gradient algorithm [34], and an inverse system method [35] were designed for the identification of a damping rate function that characterizes the non-Markovian environment in a time-convolutionless master equation. The identification can be also done in the frequency domain, where the kernel function of a non-Markovian environment is embedded in an integral-differential master equation [36]. In our previous work, we have shown that a non-Markovian environment can be modeled by using linear ancillary quantum systems where the spectrum of the environment is parametrized via a spectral factorization theorem. Hence, a non-Markovian quantum system can be modeled in an augmented Hilbert space, whose dynamics are described by a Markovian master equation [37,38]. In this paper, we assume that the dynamics of the non-Markovian quantum system with the unknown spectrum of the non-Markovian environment obey the augmented master equation. The identification of the spectrum is ascribed to estimate the parameters of the ancillary systems in the augmented system model. We apply our gradient algorithm to identify those parameters so as to recover the spectrum of the non-Markovian environment. The feasibility of our algorithm for the identification of the environment is illustrated in an example of a qubit in a non-Markovian environment with a two-Lorentzian spectrum.

This paper is organized as follows. In Sec. II, we describe the open quantum system by a master equation with unknown parameters. Then, a gradient algorithm for identification of the Markovian quantum systems is presented in Sec. III. The performance of our algorithm with both ideal and nonideal measurements is verified by an example of a quantum-dot-resonator system in Sec. IV. In Sec. V, we show that our algorithm can be applied to explore the spectrum of a non-Markovian environment. Conclusions are drawn in Sec. VI.

II. DESCRIPTION OF A MARKOVIAN QUANTUM SYSTEM WITH UNKNOWN PARAMETERS

A Markovian quantum system is referred to as a quantum system interacting with a memoryless environment, whose dynamical map obeys the semigroup property [39]. For example, the dynamics of a cavity mode interacting with a vacuum field is usually Markovian, where the field can be considered quantum white noise [39]. This kind of systems widely exists in quantum systems. Note that the definition of Markovian quantum systems here is one of existing definitions on Markovianity [40–43].

In this paper, we describe Markovian quantum systems by a master equation

$$\dot{\rho}(t) = \mathcal{L}\rho(t) = (\mathcal{L}_0 + \mathcal{L}_\theta)\rho(t), \tag{1}$$

where $\rho(t)$ is the density operator of the Markovian quantum system to be identified. Its evolution is determined by two superoperators $\mathcal{L}_0$ and $\mathcal{L}_\theta$ as shown on the right-hand side of Eq. (1). The first superoperator

$$\mathcal{L}_0\rho(t) = -i[H_0, \rho(t)] + \sum_{q=1}^{Q} \lambda_q \mathcal{D}_{L_q}\rho(t) \tag{2}$$

represents the known dynamics of the system where H_0 is the Hamiltonian of the system and $[\cdot,\cdot]$ is the commutator for two operators. The second term on the right-hand side of Eq. (2) describes the Q channels of dissipative processes with the given damping rate constants $\{\lambda_q, q = 1, \ldots, Q\}$. The Lindblad superoperator $\mathcal{D}_{L_q}$ is calculated as

$$\mathcal{D}_{L_q}\rho(t) = L_q\rho(t)L_q^\dagger - \tfrac{1}{2}L_q^\dagger L_q\rho(t) - \tfrac{1}{2}\rho(t)L_q^\dagger L_q, \quad q = 1, \ldots, Q, \tag{3}$$

with a coupling operator L_q of the system for each dissipative channel with respect to quantum white noise. Hereafter, we have assumed that Plank constant $\hbar = 1$.

The second superoperator,

$$\mathcal{L}_\theta\rho(t) = -i\left[\sum_{m=1}^{M} \theta_m H_m, \rho(t)\right] + \sum_{n=1}^{N} \theta_{M+n}\mathcal{D}_{L_n}\rho(t), \tag{4}$$

describes the unknown quantum dynamics. The first part corresponds to the unknown coherent dynamics involving M *unknown* parameters $\{\theta_m, m = 1, \ldots, M\}$ associated with M Hamiltonians. The second part represents the unknown incoherent dynamics involving N parameters $\{\theta_{M+n}, n = 1, \ldots, N\}$ associated with N Lindbladians. Here, $\mathcal{D}_{L_n}\rho(t)$ is written in the same form as Eq. (3). The Markovian master equation forms the basis for the identification task in this work.

Since the superoperator $\mathcal{L}$ is time invariant, the formal solution of master equation (1) is expressed as

$$\rho(t) = \exp\{\mathcal{L}(t - t_0)\}\rho(t_0), \tag{5}$$

where $t_0 = 0$ is the initial time of the evolution and $\rho(t_0)$ is the initial density operator. Note that in general it is difficult

to obtain an analytical expression of Eq. (5) since it involves calculating the exponential of the superoperator $\mathcal{L}$. Also, in the following calculation, we let $t_0 = 0$ for convenience.

III. A GRADIENT ALGORITHM FOR HAMILTONIAN IDENTIFICATION OF MARKOVIAN QUANTUM SYSTEMS

A. Measurement of time trace observables

To identify the unknown parameters in the Markovian master equation, we measure the time trace of a local observable O of the Markovian quantum system. We assume that we can repeatedly initialize the system to some initial state or we have many identical copies of the system. This assumption is common and can also be found in Ref. [4]. Under this assumption, we measure the observable O with an equal sampling time Δt; i.e., the time interval from an initial time 0 to a final time T can be divided into $K = T/\Delta t$ equal intervals. At a sampling time, the density matrix of the system is projected onto the basis of the observable O. With the measurement data at every sampling time, we can map the states of the Markovian quantum system to the time trace of the observable O, which can be written as

$$\hat{y} = [\hat{y}_1, \ldots, \hat{y}_k, \ldots, \hat{y}_K]^T. \tag{6}$$

Here, $\hat{y}_k$ is the real measured time trace of the observable O at the kth sampling time $t_k = k\Delta t$ with $k = 1, \ldots, K$; i.e., $\hat{y}_k$ are the measured mean values of O at the kth sampling time.

Since these real measurement results reflect the dynamics of the density matrix $\rho(t)$ affected by the unknown parameters, one can identify these unknown parameters via sufficiently many measurement observables.

B. Description of the Hamiltonian identification problem for the Markovian quantum system

Due to the measurement process, the evolution of the Markovian quantum system can be discretized. Since the parameters in master equation (1) are all constants, the dynamical map of the system obeys the semigroup property. Hence, the density matrix $\rho(t_k)$ at the time $t_k = k\Delta t$ can be calculated as

$$\rho(t_k) = \mathcal{M}_k \cdots \mathcal{M}_2 \mathcal{M}_1 \rho(0), \quad k = 1, \ldots, K, \tag{7}$$

where $\rho(0)$ is the initial density matrix of the system. The discretized superoperator of $\mathcal{L}$ is written in a matrix exponential form as

$$\mathcal{M}_\kappa = \exp\{\Delta t(\mathcal{L}_0 + \mathcal{L}_\theta)\}, \quad \kappa = 1, \ldots, k. \tag{8}$$

Further, when we guess a set of unknown parameters, using Eq. (7), we can calculate the corresponding time trace observable at the time $t_k = k\Delta t$ as

$$y = [y_1, \ \ldots, y_k, \ \ldots, y_K]^T, \tag{9}$$

where $y_k = \mathrm{tr}[O\rho(t_k)]$ are the calculated expectation values of the observable O at the kth sampling time. Although the output y is not the real measurement result, it reflects how the given set of parameters affects the output of the system, which can afford a hint for finding the real parameters.

To measure the distance between the real measurement result $\hat{y}$ and the calculated result y, we define an objective function

$$J = \frac{1}{2}\sum_{k=1}^{K}(y_k - \hat{y}_k)^2, \tag{10}$$

which is a summation of the square of the differences between the real measurement and calculated results at every sampling time.

Thus, the identification problem considered in this paper can be converted to an optimization problem as follows. Given the real measurement results $\hat{y}$ [Eq. (6)], the optimization problem is to find a set of the unknown parameters $\{\theta_1, \ldots, \theta_M, \theta_{M+1}, \ldots, \theta_{M+N}\}$ that minimizes the objective function J subject to the evolution (7).

C. A gradient algorithm for solving the optimization problem

Gradient algorithms have been proposed for solving optimization problems for quantum systems [44]. For example, it can be applied to design optimal control pulses for transferring quantum states [44]. In this paper, we design a gradient algorithm for revealing the real unknown parameters such that we can minimize the corresponding objective J. The core issue for designing the algorithm is to calculate the gradient of the objective J with respect to the unknown parameters, with which we can search for an optimal solution along the gradient descent direction.

For the convenience of the following derivation, we rewrite the unknown parameter set as $\{\theta_p, p = 1, \ldots, M+N\}$. By using the chain rule, the gradient of J with respect to the unknown parameters $\{\theta_p, p = 1, \ldots, M+N\}$ can be calculated as

$$\frac{\partial J}{\partial \theta_p} = \sum_{k=1}^{K}(y_k - \hat{y}_k)\left\langle O\frac{\partial \rho_k}{\partial \theta_p}\right\rangle. \tag{11}$$

Since the unknown parameters have been assumed to be constants in every time interval, they affect the dynamics in every time interval. Hence, the gradient of ρ_k with respect to the unknown parameters corresponds to the superoperators $\mathcal{M}_\kappa$ from the initial $\kappa = 1$ up to $\kappa = k$ time intervals, which can be calculated as

$$\frac{\partial \rho_k}{\partial \theta_p} = \sum_{\kappa=1}^{k} \mathcal{M}_k \cdots \mathcal{M}_{\kappa+1}\frac{\partial \mathcal{M}_\kappa}{\partial \theta_p}\mathcal{M}_{\kappa-1}\cdots\mathcal{M}_1\rho(0). \tag{12}$$

Further, the gradient of the discretized superoperator $\mathcal{M}_\kappa$ with respect to the unknown parameters can be approximated as

$$\frac{\partial \mathcal{M}_\kappa}{\partial \theta_p} \approx \begin{cases} \Delta t\mathcal{L}_m(\cdot)\mathcal{M}_\kappa(\cdot), & p = 1, \ldots, M \\ \Delta t\mathcal{D}_{L_n}(\cdot)\mathcal{M}_\kappa(\cdot), & p = M+1, \ldots, M+N, \end{cases} \tag{13}$$

where the superoperator $\mathcal{L}_m$ is defined as $\mathcal{L}_m(\cdot) = -i[H_m, (\cdot)]$. The superoperators $\mathcal{D}_{L_n}$ and $\mathcal{M}_\kappa$ can be computed as Eqs. (3) and (8), respectively.

By utilizing Eqs. (11)–(13), we can update the guessed unknown parameters as

$$\theta_p \to \theta_p - \epsilon\frac{\partial J}{\partial \theta_p}, \tag{14}$$

where ϵ is the positive step size. Note that we update the parameters along their descent gradient directions and thus the corresponding updated objective function can be smaller than the original one.

We summarize the gradient identification algorithm for the Markovian quantum system as follows:

(1) Choose a local observable O, measure the time trace of the observable $\hat{y}$, initialize the state of the system $\rho(0)$ and the step size ϵ, and guess the initial values of the unknown parameters.

(2) Calculate the evolution of the density matrices of the Markovian quantum system from $\rho(1)$ to $\rho(K)$ and the outputs from y_1 to y_K with the guessed unknown parameters.

(3) Compute the objective J and its gradient with respect to $\{\theta_p\}$ according to Eqs. (11)–(13).

(4) Update θ_p using relation (14).

(5) When a termination condition is satisfied, stop the algorithm; otherwise, go to step 2 and start a new iteration.

Importantly, our algorithm is designed for a general Markovian quantum system, where we have not specified the Hamiltonian of the system. Compared to the existing identification methods working for either finite-level quantum systems or infinite-level quantum systems, our algorithm works for a general Markovian quantum system involving both of them.

Note that in our algorithm we only require that the identified parameters satisfy condition (10). Hence, Eq. (10) is a necessary condition for the identification problem. This means that multiple estimates would result in the same objective function (10) as indicated in Ref. [12]. To make sure the optimized parameters are the real ones, we should run our algorithm several times with randomly chosen initial values of the unknown parameters in the parameter space. When the same local minimum can be achieved by our algorithm with the randomly chosen initial values, we say that the optimized parameters can achieve a local minimum in a subspace of the parameters. When the number of the initial values is sufficiently large, we can consider the local minimum is global and the identified parameters are real. As pointed out in Ref. [18], these additional resources for identification would help with the multiple estimates issue.

IV. IDENTIFICATION OF UNKNOWN PARAMETERS IN A QUANTUM-DOT-RESONATOR SYSTEM

A. Description of a quantum-dot-resonator system

In this example, we test the performance of our algorithm by a quantum-dot-resonator system [2] where the charged quantum dot and the resonator are both dissipative. This system can be described by an open Jaynes-Cummings model which is widely used in circuit or cavity quantum electrodynamical systems [29,30].

The Hamiltonian of this system can be written as

$$H = \frac{\nu_q}{2}\sigma_z + \nu_0 a^\dagger a + g_d(a^\dagger\sigma_- + a\sigma_+), \tag{15}$$

where the first two terms on the right-hand side are the internal Hamiltonian of the quantum dot and the resonator, respectively, and the third term describes the interaction between them. σ_z is the z-axis Pauli matrix and σ_- and σ_+ are the ladder operators for the quantum dot. The annihilation and creation operators of the resonator are written as a and $a^\dagger$, respectively. The Hamiltonian involves three parameters: the splitting frequency of the quantum dot, ν_q; the angular frequency of the resonator, ν_0; and the coupling strength between them, g_d. In addition, the coupling operators of the quantum dot and the resonator for each dissipative channel are $L_1 = \sigma_-$ and $L_2 = a$, respectively. Hence, the dynamics of this open system can be described by a master equation as

$$\begin{aligned}\dot{\rho}(t) = &-i\left[\frac{\nu_q}{2}\sigma_z + \nu_0 a^\dagger a + g_d(a^\dagger\sigma_- + a\sigma_+), \rho(t)\right] \\ &+\gamma_d\left(\sigma_-\rho(t)\sigma_+ - \frac{1}{2}\sigma_+\sigma_-\rho(t) - \frac{1}{2}\rho(t)\sigma_+\sigma_-\right) \\ &+\gamma_0\left(a\rho(t)a^\dagger - \frac{1}{2}a^\dagger a\rho(t) - \frac{1}{2}\rho(t)a^\dagger a\right).\end{aligned} \tag{16}$$

TABLE I. Four guessed initial values for the unknown parameters.

Labels	g_{d0}	γ_{d0}	ν_{q0}
Ex1Set1	0.6 GHz	0.1π GHz	3 GHz
Ex1Set2	0.2 GHz	0.15π GHz	7 GHz
Ex1Set3	0.5 GHz	0.05π GHz	5 GHz
Ex1Set4	0.4 GHz	0.25π GHz	4 GHz

B. Identification of unknown parameters with error-free measurement results

In this paper, we assume that the splitting frequency of the quantum dot, ν_q, the coupling strength g_d, and the damping rate γ_d are unknowns to be identified. We adopt the parameters for the quantum-dot-resonator system in Ref. [2] to simulate the dynamics of the real system. We set $\nu_0 = 6.775$ GHz, $\nu_q = 6.1814$ GHz, $g_d = 0.3142$ GHz, $\gamma_d = 0.6283$ GHz, and $\gamma_0 = 2.6\times 2\pi$ MHz. With these parameters, we can simulate the real measurement result $\hat{y}$ where the observable σ_x of the quantum dot is measured; i.e., the measurement result is error free. We sample the observable σ_x for one thousand times in a total time 1 ns.

To start, we randomly choose initial guesses on the unknown parameters given in Table I. The step sizes for updating the three parameters are 0.0002 GHz and the termination condition is that the algorithm achieves 40 000 iterations. We assume that the quantum dot and the resonator are initialized on the state $\frac{1}{2}(I + \sigma_x)$ and the ground state, respectively. Note that we have truncated the infinite levels of the resonator to 20 levels to obtain the real measurement results in the simulation and 8 levels in the identification model, respectively. The identification result is further examined by truncating the oscillator to 20 levels to make sure the 8-level truncation is sufficient. Simulation results show that they are consistent. If not, one can gradually increase the number of levels and use the obtained identification as an initial guess to refine the optimization.

The convergence for the three parameters is given in Fig. 1. In the cases of four initial guesses, the values of the unknown parameters approach their real ones, where the converging process of the splitting frequency ν_q is very fast compared

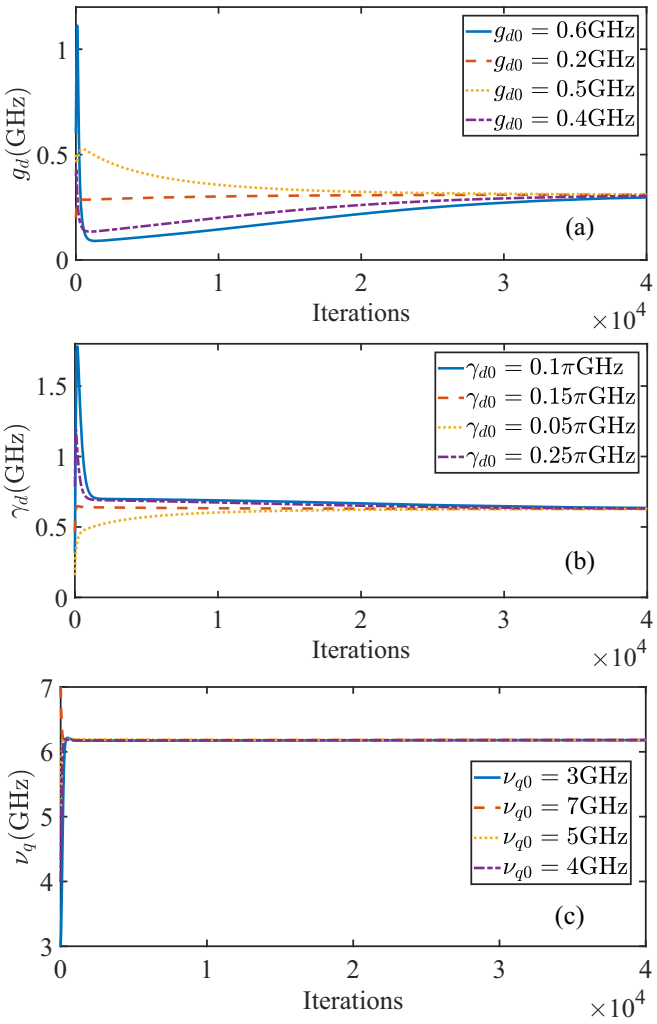

FIG. 1. The convergence processes for the identified unknown parameters: (a) the coupling strength g_d, (b) the damping rate γ_d, and (c) the splitting frequency ν_q with four sets of the initial guessed values. The three parameters in the four cases all approach their real values by using our gradient identification algorithm.

with the slow ones for the other two parameters. It shows that our algorithm can iteratively learn the real values of the unknown parameters by utilizing the measurement results on the expectation values of the observable σ_x as shown in Fig. 1. The variation of the corresponding objective function J during the identification process is shown in Fig. 2. As the identified values of the unknown parameters approach the real values, the objective functions J decrease monotonically. The objective J is reduced down to 10^{-7} with the second initial guess which is lower than all other cases. The best identified values for the three parameters are $\hat{g}_d = 0.3097$ GHz, $\hat{\gamma}_d = 0.6285$ GHz, and $\hat{\nu}_q = 6.1814$ GHz. These results illustrate that our identification algorithm can achieve a high precision for the identification with suitable initial guesses.

The above simulation shows that our algorithm can identify the unknown parameters in a Markovian quantum-dot-resonator system with a high precision by using only the measurement results of a local observable. Although the

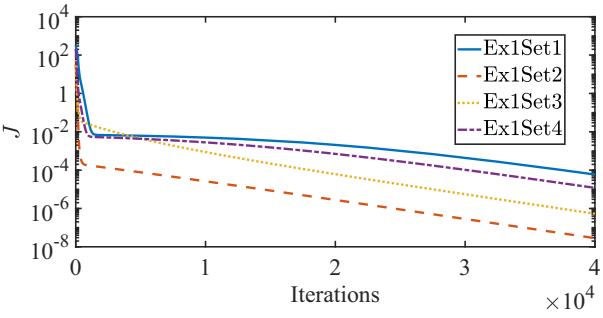

FIG. 2. The convergence of the objective J in the cases of four initial guessed values of the unknown parameters for the quantum-dot-resonator system. With the suitable initial guess, our gradient identification algorithm can achieve a high precision for the identification.

algorithm involves an iterative searching process costing computational time, it is acceptable since this process is offline.

C. Identification of unknown parameters with low-sampled or noisy measurement results

In the above section, the corresponding identification results are obtained based on error-free measurements. However, this ideal case would not happen in an experiment. Hence, it is necessary to verify the performance of our algorithm in some practical cases. In this section, we consider two practical cases. One is low-sampled measurements, and the other one is noisy measurements.

Case of low-sampled measurements. In this case, we consider that the number of sampled time traces K is not sufficient. Concretely, we measure $K = 50$, 100, 200, and 500 samples for time traces with which we observe the impact of low-sampled data on the identification results. With these low-sampled measurements, we also identify the three parameters as in Sec. IV B. We keep all parameters and the initial state of the system and the settings in our algorithm identical to that in Sec. IV B. We also start our algorithm with the guessed initial values of the unknown parameters as given in Table I.

The variations of the objective J with respect to the different K are plotted in Fig. 3, where the four panels correspond to the results with the guessed parameters as in Table I. We observe that our algorithm achieves low identification accuracies with low-sampled measurements. Similar to the results in Sec. IV B, good guessed initial values of the parameters lead to a high identification accuracy. For example, the final objective as given in Fig. 3(b) is less than those in other parts of Fig. 3.

Correspondingly, we plot the errors

$$e = \left|\frac{\hat{\phi} - \phi}{\phi}\right| \times 100\% \tag{17}$$

for the identified parameters obtained by our algorithm with low-sampled measurements in Fig. 4, where $\hat{\phi}$ and ϕ represent the identified and nominal values of the corresponding parameters, respectively. The errors of the identified parameters can be reduced when the number of sampled time traces is increased. For the frequency ν_q, even with

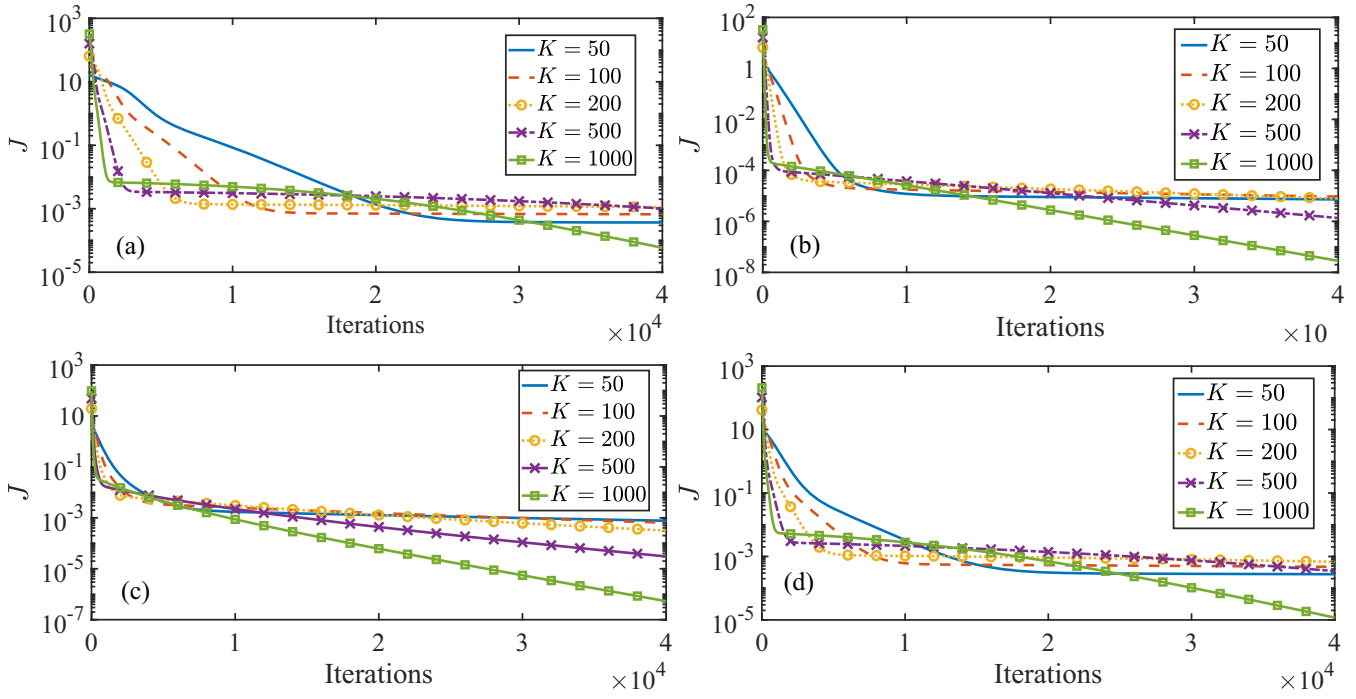

FIG. 3. Variation of the objective J with the different numbers of the sampled datafor the different initial guesses in Table I with the labels (a) Ex1Set1, (b) Ex1Set2, (c) Ex1Set3, and (d) Ex1Set4.

low-sampled data, e.g., $K = 50$, our algorithm can identify its value with an error lower than 0.2%. However, the low-sampled data result in huge errors for the parameter g_d plotted as blue stars in Fig. 4. This shows that part of the identified parameters can be sensitive to low sampling frequencies. Hence, to precisely calibrate parameters of a system in an experiment using our algorithm, it would be better to utilize measurements as much as possible.

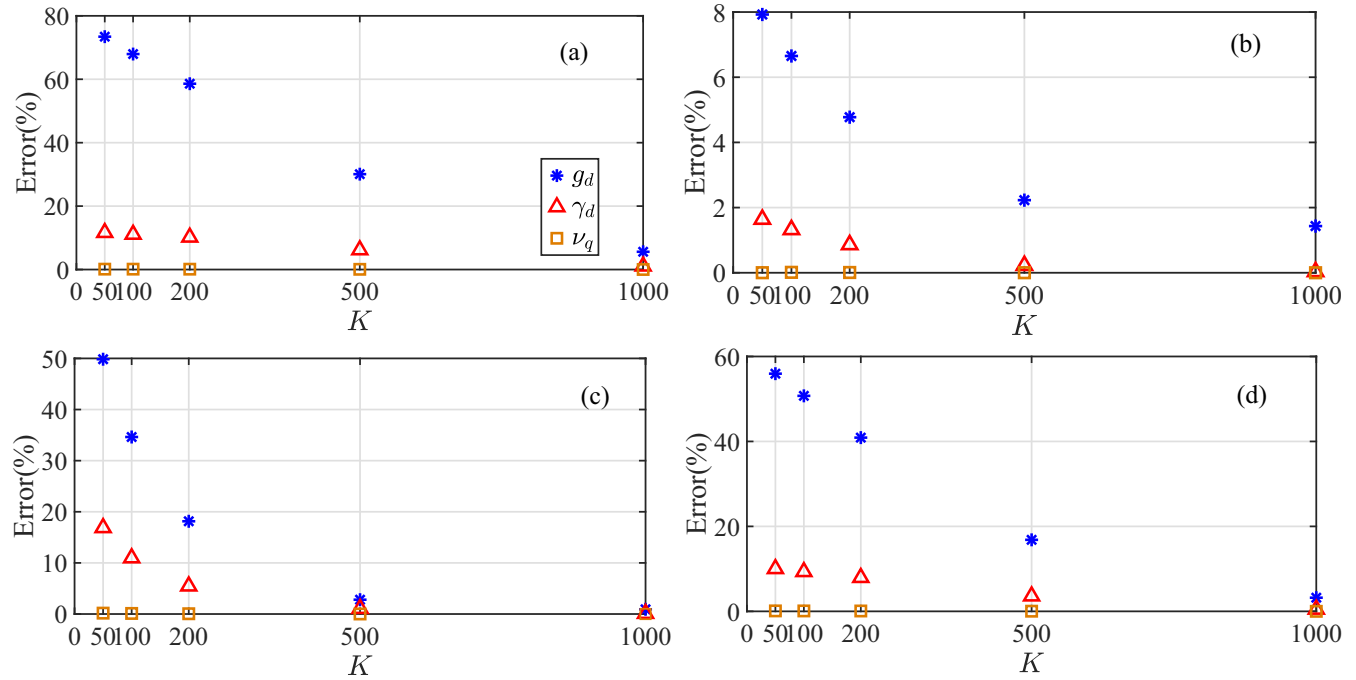

FIG. 4. Errors of the identified parameters with the number of sampled data K, corresponding to the different initial guesses in Table I with the labels (a) Ex1Set1, (b) Ex1Set2, (c) Ex1Set3, and (d) Ex1Set4, respectively. Blue stars, red triangles, and brown squares represent the identified results for g_d, γ_d, and ν_q, respectively.

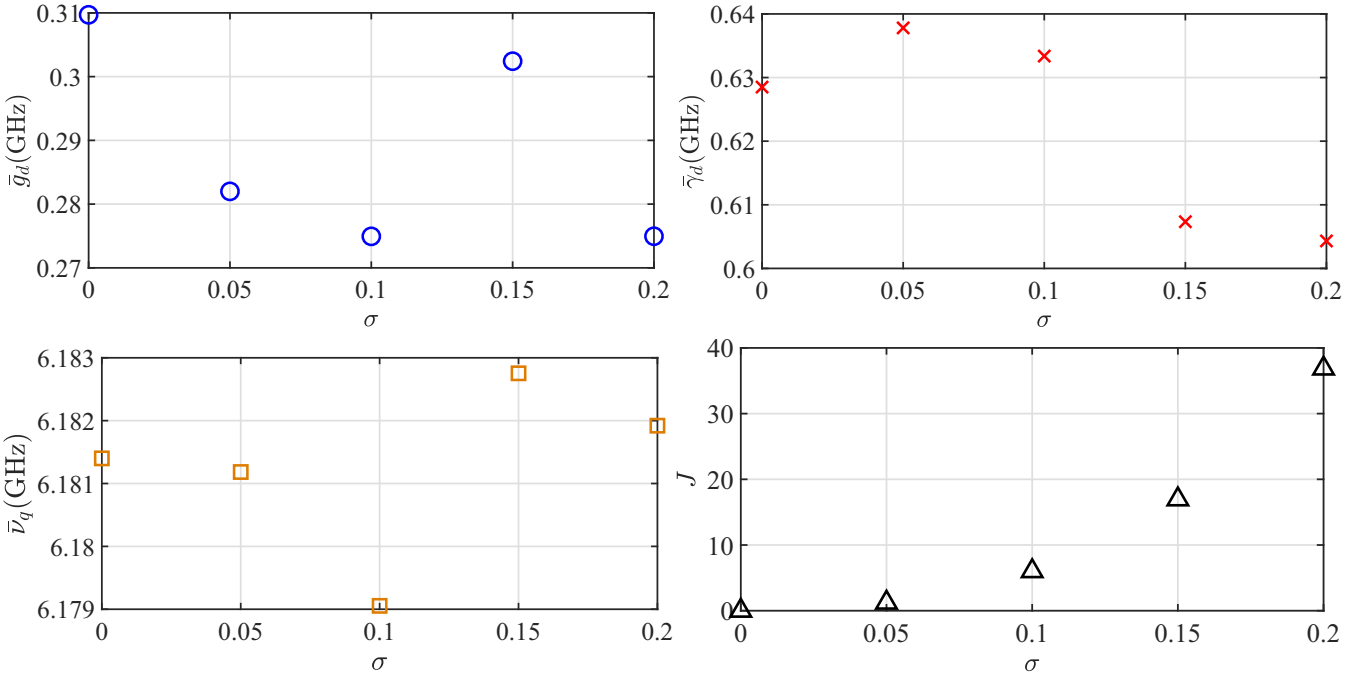

FIG. 5. Averaged identified unknown parameters and objective J with respect to the different standard deviation σ of the Gaussian noise. The increasing standard deviation σ of the Gaussian noise results in the errors of the corresponding parameters and the increasing of the objective.

Case of noisy measurements. In this case, we explore the impact of measurement noises on the identification results. Although the effect of noises can be averaged out by measuring observables with infinite samples in principle, it should be considered due to finite samples in an experiment. Hence, the robustness of our algorithm to noise is investigated.

We consider the same system as that in Sec. IV B. We also equally measure the time traces of the observable σ_x 1000 times in the total time. Suppose that these measurement results are polluted by additive Gaussian noise as

$$\hat{y}_k^{\text{noisy}} = \hat{y}_k + \zeta_k, \tag{18}$$

where $\zeta_k \sim \mathcal{N}(0, \sigma^2)$ for all k with zero mean and standard deviation σ. We set $\sigma = 0.05$, 0.1, 0.15, and 0.2 and also consider $\sigma = 0$ for the noiseless case. We generate the noisy measurements and run our algorithm for identification of the three parameters 40 times. For each time, we run our algorithm for 40 000 iterations. We average over these identification results and plot the identification results with respect to the standard deviations in Fig. 5, where the corresponding averaged parameters are denoted with a bar.

As shown in Fig. 5, due to the effect of noise, the values of the identified parameters deviate from their real values and thus the accuracy of the identification results obtained from the noisy measurements is less than that in the noise-free case. This is shown in the bottom right panel of Fig. 5 for the objective J. As the standard deviation σ of the Gaussian measurement noise increases, the objective J is increased. This result indicates that it becomes difficult to estimate the real values of the parameters using our algorithm when the standard deviation of the noise is large.

V. IDENTIFICATION OF A NON-MARKOVIAN ENVIRONMENT FOR A QUBIT SYSTEM

A. An augmented Markovian system model of a non-Markovian qubit

In actual systems, a quantum information carrier involving complicated interactions would exhibit non-Markovian dynamics [41,45,46]. The complicated interactions can be explained as the influence of a non-Markovian environment which is characterized by a noise spectrum $S(\omega)$. The non-Markovian dynamics of the system can be described by an integral-differential quantum Langevin equation, where the noise spectrum of the environment embedded in a memory kernel function determines the non-Markovian dynamics. For more details, see Refs. [31,47]. In this paper, we consider the non-Markovian system described by the integral-differential quantum Langevin equation as the original system of interest whose schematic plot is given in Fig. 6. The noise spectrum of the environment in the Langevin equation is to be identified from the measurement data of the system. This identification problem is important for obtaining a suitable model for the aim of control. Similar ideas using a qubit as a probe can be found in recent works [48–51].

For the purpose of identification, we need to represent the original system as an augmented system model which has been presented in our previous works [37,38]. In the augmented system model as shown in Fig. 6, a principal system and an ancillary system represent the original quantum system and the non-Markovian environment, respectively. The ancillary system consisting of several one-mode quantum harmonic oscillators driven by quantum white noise is used to capture the effective modes of the non-Markovian environment indicated by the noise spectrum $S(\omega)$. For each

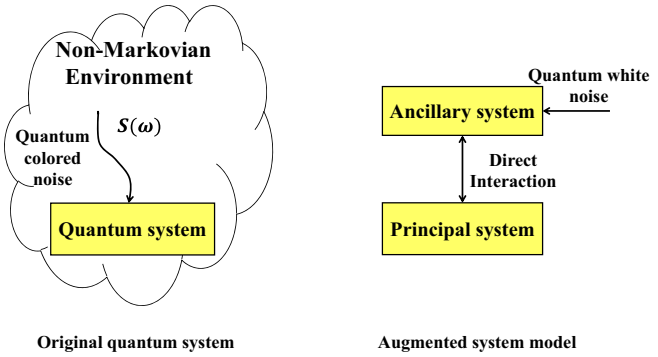

FIG. 6. A schematic plot of the augmented system model for a non-Markovian quantum system. The original quantum system and the non-Markovian environment are represented by a principal system and an ancillary system, respectively, in the augmented system model.

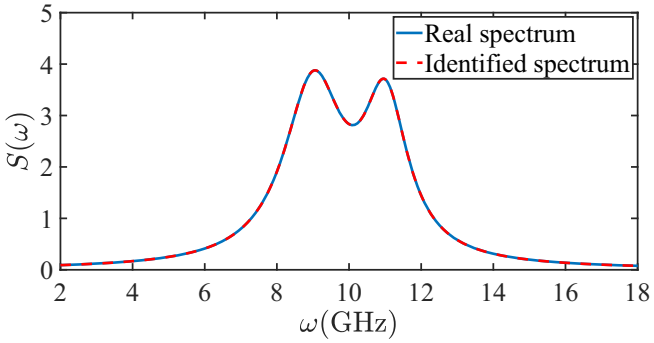

FIG. 7. The real and identified two-Lorentzian spectra which are plotted as the solid blue and dashed red lines, respectively. The identified spectrum obtained by using our gradient algorithm matches the real one.

oscillator, a fictitious output is defined, whose power spectral density is Lorentzian [37]. The center frequency, the width, and the strength of the Lorentzian spectrum are determined by the angular frequency ω_r, the damping rate with respect to the quantum white noise, $\sqrt{\bar{\gamma}_r}$, and the coupling strength to the principal system of the quantum harmonic oscillator, $\sqrt{\beta_r}$, respectively. Coupling these ancillary systems to the same operator of the principal system via their direct interactions, the combination of the Lorentzian spectra can approximate noise with an arbitrary spectrum; i.e.,

$$S(\omega) \approx \sum_r \frac{\beta_r \frac{\bar{\gamma}_r^2}{4}}{\frac{\bar{\gamma}_r^2}{4} + (\omega - \omega_r)^2}. \tag{19}$$

Here, the operator of the principal system is chosen for reproducing the quantum Langevin equation of the original system [37]. The direct interactions can capture the mutual influence between the non-Markovian environment and the system. In this augmented system model, the dynamics of the principal system also satisfy an integral-differential quantum Langevin equation which is consistent with that of the original system (see Eq. (27) in Ref. [37] for more details). In this sense, we can take the augmented system model as a model of the original system for identification.

In this section, we couple a single-qubit system to a non-Markovian environment such that the results of the measurement on the qubit can help to access the information of the environment. For the purpose of identification, we take the augmented system model as the model of the original system, where the information of the environment corresponds to the parameters of the ancillary system.

Since the quantum colored noise is whitened by the ancillary system, the augmented system is driven by quantum white noise such that the dynamics of the augmented system can be described by a Markovian master equation [37,38]

$$\dot{\rho}(t) = (\mathcal{L}_q + \mathcal{L}_i + \mathcal{L}_d)\rho(t), \tag{20}$$

where $\rho(t)$ is the density matrix of the augmented system. The superoperator

$$\mathcal{L}_q\rho(t) = -i[H_q, \rho(t)] \tag{21}$$

describes the internal dynamics of the principal system. The Hamiltonian of the qubit is $H_q = \frac{1}{2}\omega_0\sigma_z$ with a working frequency ω_0. Moreover, we represent the environment by using many one-mode oscillators so that the internal dynamics of the ancillary systems and the dynamics induced by their couplings to the principal system are described by the superoperator

$$\mathcal{L}_i\rho(t) = -i\left[\sum_{r=1}^{R}\omega_r a_r^\dagger a_r + \sum_{r=1}^{R} i\mu_r(a_r^\dagger\sigma_- - \sigma_+ a_r), \rho(t)\right], \tag{22}$$

where the operators a_r and $a_r^\dagger$ and the frequency ω_r are the annihilation and creation operators and the angular frequency for the rth ancillary system, respectively. The annihilation and creation operators satisfy the canonical commutation relation [39]. We have defined the fictitious output of each ancillary system as $c_r = -\frac{\sqrt{\bar{\gamma}_r}}{2}a_r$, which is coupled to the principal system through an operator $\sqrt{\beta_r}\sigma_-$ via their direct interaction $i\mu_r(a_r^\dagger\sigma_- - \sigma_+ a_r)$ with a coupling strength $\mu_r = -\frac{\sqrt{\bar{\gamma}_r\beta_r}}{2}$. Here, $\bar{\gamma}_r$ is the damping rate of the rth ancillary system with respect to quantum white noise and β_r is the coupling strength between the principal system and the rth ancillary system. It has been shown that the fictitious output c_r carries a channel of quantum Lorentzian noise. Since they have been coupled to the same operator of the principal system z_*, we can combine these Lorentzian noises for

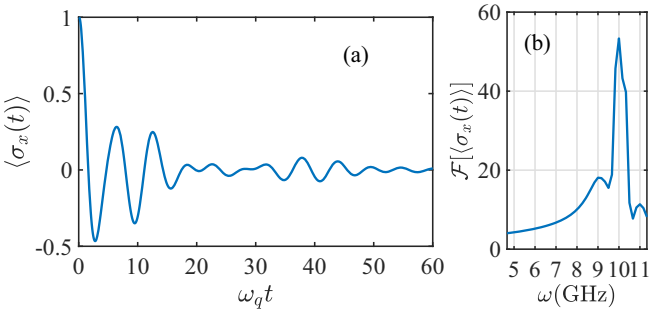

FIG. 8. The evolution of the expectation value of the observable σ_x and its corresponding Fourier transform. The Fourier transform of the output indicates the number of the ancillary system.

TABLE II. Six guessed initial values for the unknown parameters.

Labels	ω_1^0	ω_2^0	μ_1^0	μ_2^0	γ_1^0	γ_2^0
Ex2Set1	9.40 GHz	10.80 GHz	−1.45 GHz	−1.07 GHz	1.56 GHz	1.92 GHz
Ex2Set2	8.50 GHz	11.50 GHz	−1.20 GHz	−0.95 GHz	2.50 GHz	1.00 GHz
Ex2Set3	10.00 GHz	12.00 GHz	−2.00 GHz	−1.30 GHz	3.00 GHz	1.40 GHz
Ex2Set4	8.00 GHz	10.50 GHz	−1.00 GHz	−0.90 GHz	1.80 GHz	2.00 GHz
Ex2Set5	9.20 GHz	11.80 GHz	−1.50 GHz	−1.10 GHz	1.40 GHz	1.60 GHz
Ex2Set6	8.40 GHz	11.30 GHz	−1.30 GHz	−0.80 GHz	2.00 GHz	2.20 GHz

generating quantum colored noise with one arbitrary spectrum. In addition, the dissipative processes of the ancillary systems with respect to quantum white noise are described by the superoperator

$$\mathcal{L}_d\rho(t) = \sum_{r=1}^{R} \bar{\gamma}_r \mathcal{D}_{L_r}\rho(t), \tag{23}$$

where $L_r = a_r$ is the coupling operator of the rth ancillary system.

Note that with this augmented system model, we can represent a non-Markovian quantum system in a high-dimensional Hilbert space as a Markovian quantum system, where the augmented system is only driven by quantum white noise. In the Heisenberg picture, our augmented system model can reproduce the traditional integral-differential Langevin equation [37]. In this sense, the augmented system model is consistent with the traditional model. Also, the quantum colored noise arising in the non-Markovian environment is whitened, whose noise spectrum is parametrized by the ancillary system. Hence, this augmented system model forms the bases for identification of the non-Markovian environment.

B. Identification of the non-Markovian environment of a qubit

We consider that the real noise spectrum $S(\omega)$ of the non-Markovian environment for a qubit system is in a

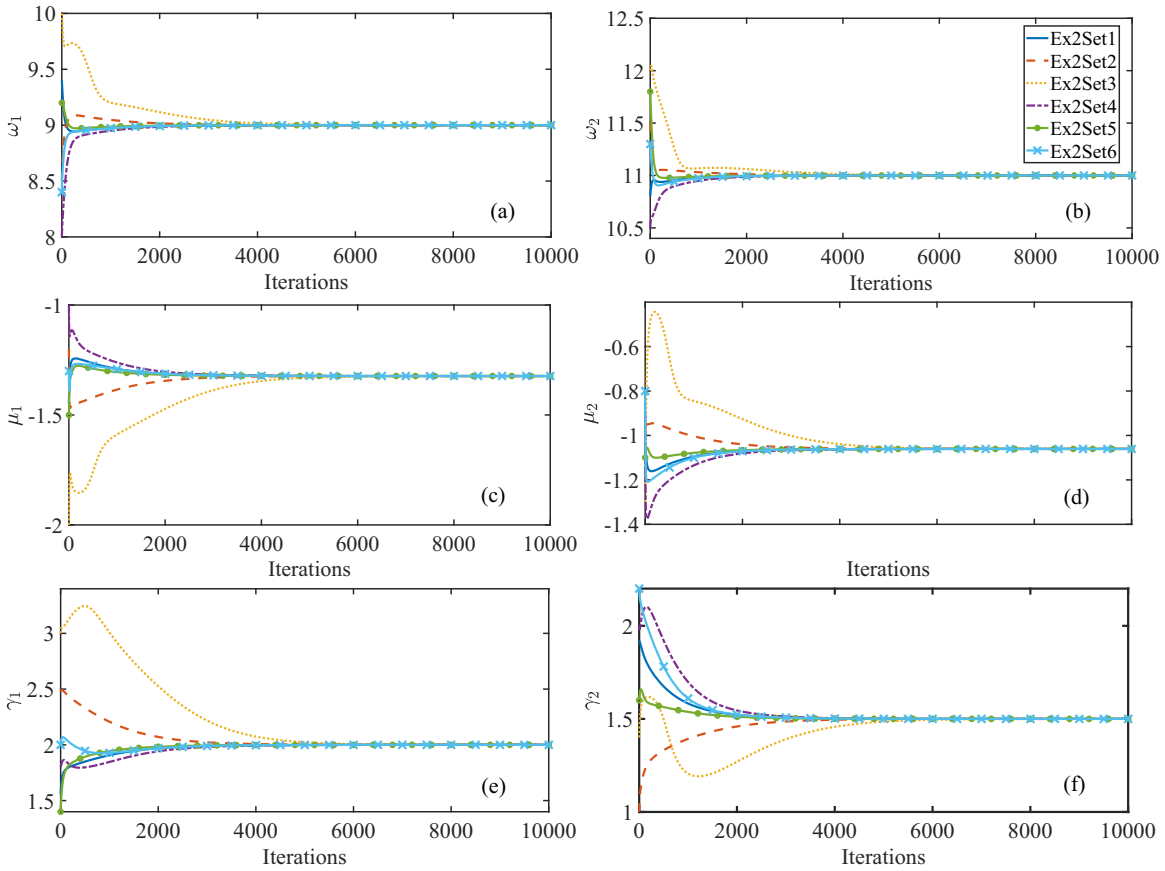

FIG. 9. Variations of the identified parameters (a) ω_1, (b) ω_2, (c) μ_1, (d) μ_2, (e) γ_1, and (f) γ_2 of the ancillary systems in the augmented system model. The final results are close to the real values.

two-Lorentzian shape [39] as

$$S(\omega) = \frac{\beta_1\left(\frac{\bar{\gamma}_1}{2}\right)^2}{\left(\frac{\bar{\gamma}_1}{2}\right)^2 + (\omega-\omega_1)^2} + \frac{\beta_2\left(\frac{\bar{\gamma}_2}{2}\right)^2}{\left(\frac{\bar{\gamma}_2}{2}\right)^2 + (\omega-\omega_2)^2}. \quad (24)$$

The center frequencies of the two-Lorentzian spectrum are $\omega_1 = 9$ GHz and $\omega_2 = 11$ GHz, respectively. The widths of the spectrum are $\bar{\gamma}_1 = 2$ GHz and $\bar{\gamma}_2 = 1.5$ GHz and their strengthes are determined by $\beta_1 = 3.5$ GHz and $\beta_2 = 3$ GHz, respectively. This spectrum plotted as the blue line in Fig. 7 is used to characterize the real non-Markovian environment which induces the non-Markovian dynamics of a qubit with an angular frequency $\omega_0 = 10$ GHz. We sample the observable σ_x 1000 times in a total time of 6 ns.

We initialize the qubit in the state $\frac{1}{2}(I + \sigma_x)$. In our simulation, we assume that the ancillary systems are initialized in the ground states. Note that we also truncate the infinite levels of the ancillary linear quantum system to eight levels. For this system, we simulate the real measurement result using the expectation of the local observable σ_x of the qubit.

Before running the gradient identification algorithm, the number of ancillary systems must be determined. Generally, non-Markovian environments are complicated such that it is difficult to obtain the exact number of ancillary systems. However, since the measured expectation values are affected by the system and its environments, the measurements carry their mode information and thus the Fourier transform of the measurements can reflect the number of effective modes in the system and its environment. Hence, we can use the Fourier transform to guess the number of the ancillary system. We can initially let the number of ancillary systems be the number of peaks in the spectrum except the peak for the principal system. And thus we can use our algorithm to identify the parameters of the ancillary systems. When satisfactory identification results are obtained, we can stop the identification procedure. Otherwise, we should increase the number of ancillary systems until a good identification result is obtained. Note that we require that the frequencies of the ancillary systems are nondegenerate when we use the discrete Fourier transform method.

To this aim, we plot the evolution of the expectation of σ_x and its corresponding discrete Fourier transform in Figs. 8(a) and 8(b), respectively. In Fig. 8(b), the curve shows that there are two additional modes beside the qubit mode, which indicates that two linear ancillary systems should be coupled to the qubit in the augmented system model. The two additional peaks are around 9 and 11 GHz. We also randomly choose the initial values of the parameters in the two ancillary systems as shown in Table II, where the superscript 0 represents their initial values. Note that in the interaction Hamiltonian the coupling strengths can be redefined as $\mu_1 = -\sqrt{\beta_1\bar{\gamma}_1}/2$ and $\mu_2 = -\sqrt{\beta_2\bar{\gamma}_2}/2$ and thus the interaction Hamiltonian can be written as $i\mu_1(a_1^\dagger\sigma_- - \sigma_+a_1)$ and $i\mu_2(a_2^\dagger\sigma_- - \sigma_+a_2)$. Hence, the task for identification of the parameters β_1 and β_2 can be converted to that for μ_1 and μ_2, respectively.

Hence, in the identification process, we can utilize the values of μ_1 and μ_2 to calculate β_1 and β_2. The step sizes for updating these parameters in our algorithm are all 0.002 GHz.

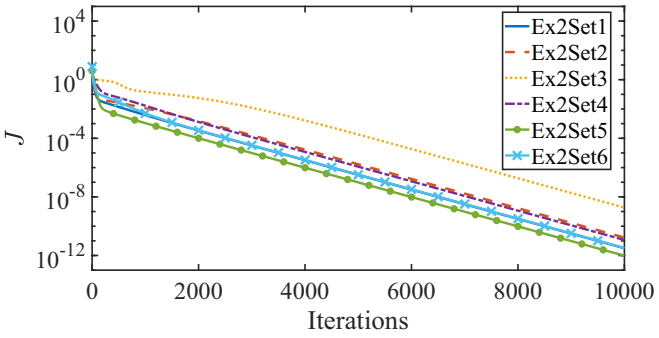

FIG. 10. Variation of the objective J when we identify the unknown parameters for the non-Markovian environment.

We run the identification algorithm for 10 000 iterations and the identification results are given in Figs. 9 and 10. With six different initial values of the parameters, the identified parameters approach the real ones. The objective function J is reduced down to 10^{-8}, which is shown in Fig. 10. The best identified frequencies and the damping rate constants are $\hat{\omega}_{1d} = 9.0000$ GHz, $\hat{\omega}_{2d} = 11.0000$ GHz and $\hat{\gamma}_{1d} = 2.0000$ GHz, $\hat{\gamma}_{2d} = 1.5000$ GHz, respectively. From the results for μ_1 and μ_2, we can obtain $\hat{\beta}_{1d} = 3.5001$ GHz and $\hat{\beta}_{2d} = 3.0002$ GHz. With respect to the best identified parameters, we plot the identified spectrum in Fig. 7 as the dashed red line, which matches the real spectrum.

VI. CONCLUSION

In this paper, we have designed a gradient algorithm for the identification of unknown parameters in open quantum systems. This algorithm can utilize the measured data of the time trace observables of the open quantum systems to iteratively learn the real values of the unknown parameters with high accuracies. We verified the performance of the gradient algorithm in the example of the quantum-dot-resonator system and applied it to identifying the non-Markovian environment based on the augmented system model. This algorithm works for a more general Markovian quantum system, which are important in the calibration of parameters of devices in an experiment with a high accuracy or to explore the interactions between a quantum system and its environment.

ACKNOWLEDGMENTS

This work was supported in part by the National Natural Science Foundation of China under Grants No. 61873162, No. 61473199, No. 61803389, and No. 61973317, in part by the Shanghai Pujiang Program under Grant No. 18PJ1405500, in part by the Suzhou Key Industry Technology Innovation Project SYG201808, in part by the Key Laboratory of System Control and Information Processing in Ministry of Education of China Scip201804, and in part by the Open Research Project of the State Key Laboratory of Industrial Control Technology, Zhejiang University, China, No. ICT1900304.

[1] M. A. Nielsen and I. L. Chuang, *Quantum Computation and Quantum Information* (Cambridge University Press, Cambridge, UK, 2000).

[2] T. Frey, P. J. Leek, M. Beck, A. Blais, T. Ihn, K. Ensslin, and A. Wallraff, Phys. Rev. Lett. **108**, 046807 (2012).

[3] J. M. Geremia and H. Rabitz, Phys. Rev. Lett. **89**, 263902 (2002).

[4] S. G. Schirmer, A. Kolli, and D. K. L. Oi, Phys. Rev. A **69**, 050306(R) (2004).

[5] M. Zhang, W. W. Zhou, H. Y. Dai, M. Lin, Z. Q. Sun, and E. L. Gong, Commun. Theor. Phys. **53**, 1077 (2010).

[6] D. D'Alessandro, IEEE Trans. Autom. Control **50**, 1054 (2005).

[7] F. Albertini and D. D'Alessandro, Linear Algebra Appl. **394**, 237 (2005).

[8] D. Burgarth and K. Maruyama, New J. Phys. **11**, 103019 (2009).

[9] D. Burgarth, K. Maruyama, and F. Nori, New J. Phys. **13**, 013019 (2011).

[10] C. Di Franco, M. Paternostro, and M. S. Kim, Phys. Rev. Lett. **102**, 187203 (2009).

[11] E. H. Lapasar, K. Maruyama, D. Burgarth, T. Takui, Y. Kondo, and M. Nakahara, New J. Phys. **14**, 013043 (2012).

[12] D. Burgarth and K. Yuasa, Phys. Rev. Lett. **108**, 080502 (2012).

[13] S. Bonnabel, M. Mirrahimi, and P. Rouchon, Automatica **45**, 1144 (2009).

[14] Z. Leghtas, G. Turinici, H. Rabitz, and P. Rouchon, IEEE Trans. Autom. Control **57**, 2679 (2012).

[15] S. G. Schirmer and D. K. L. Oi, Phys. Rev. A **80**, 022333 (2009).

[16] M. Mohseni and A. T. Rezakhani, Phys. Rev. A **80**, 010101(R) (2009).

[17] Y. Wang, D. Dong, B. Qi, J. Zhang, I. R. Petersen, and H. Yonezawa, IEEE Trans. Autom. Control **63**, 1388 (2018).

[18] J. Zhang and M. Sarovar, Phys. Rev. Lett. **113**, 080401 (2014).

[19] S.-Y. Hou, H. Li, and G.-L. Long, Sci. Bull. **62**, 863 (2017).

[20] J. Zhang and M. Sarovar, Phys. Rev. A **91**, 052121 (2015).

[21] W. W. Zhou, S. Schirmer, E. L. Gong, H. W. Xie, and M. Zhang, Chin. Sci. Bull. **57**, 2242 (2012).

[22] M. Guta, Phys. Rev. A **83**, 062324 (2011).

[23] C. Catana, T. Kypraios, and M. Guta, J. Phys. A: Math. Theor. **47**, 415302 (2014).

[24] H. Mabuchi, Quantum Semiclass. Opt. **8**, 1103 (1996).

[25] Z. Xue, H. Lin, and T. H. Lee, IEEE Trans. Autom. Control **58**, 1805 (2013).

[26] Y. Kato and N. Yamamoto, New J. Phys. **16**, 023024 (2014).

[27] M. Guta and N. Yamamoto, IEEE Trans. Autom. Control **61**, 921 (2016).

[28] M. Levitt and M. Guta, Phys. Rev. A **95**, 033825 (2017).

[29] A. Wallraff, D. I. Schuster, A. Blais, L. Frunzio, R.-S. Huang, J. Majer, S. Kumar, S. M. Girvin, and R. J. Schoelkopf, Nature **431**, 162 (2004).

[30] X. Mi, J. V. Cady, D. M. Zajac, P. W. Deelman, and J. R. Petta, Science **355**, 156 (2017).

[31] S. B. Xue, R. B. Wu, W. M. Zhang, J. Zhang, C. W. Li, and T. J. Tarn, Phys. Rev. A **86**, 052304 (2012).

[32] S. Xue, R. Wu, M. R. Hush, and T.-J. Tarn, Quantum Sci. Technol. **2**, 014002 (2017).

[33] B. Bellomo, A. De Pasquale, G. Gualdi, and U. Marzolino, Phys. Rev. A **82**, 062104 (2010).

[34] S. Xue, J. Zhang, and I. R. Petersen, IEEE Trans. Control Syst. Technol. **27**, 2574 (2019).

[35] S. Xue, L. Tan, R. Wu, M. Jiang, and I. R. Petersen, Phys. Rev. A **102**, 042227 (2020).

[36] R. B. Wu, T. F. Li, A. G. Kofman, J. Zhang, Y.-X. Liu, Y. A. Pashkin, J.-S. Tsai, and F. Nori, Phys. Rev. A **87**, 022324 (2013).

[37] S. Xue, M. R. Hush, and I. R. Petersen, IEEE Trans. Control Syst. Technol. **25**, 1552 (2017).

[38] S. Xue, T. Nguyen, M. R. James, A. Shabani, V. Ugrinovskii, and I. R. Petersen, IEEE Trans. Control Syst. Technol. **28**, 2564 (2020).

[39] H. P. Breuer and F. Petruccione, *The Theory of Open Quantum Systems* (Oxford University Press, Oxford, UK, 2002).

[40] Á. Rivas, S. F. Huelga, and M. B. Plenio, Rep. Prog. Phys. **77**, 094001 (2014).

[41] H.-P. Breuer, E.-M. Laine, J. Piilo, and B. Vacchini, Rev. Mod. Phys. **88**, 021002 (2016).

[42] I. de Vega and D. Alonso, Rev. Mod. Phys. **89**, 015001 (2017).

[43] L. Li, M. J. Hall, and H. M. Wiseman, Phys. Rep. **759**, 1 (2018).

[44] N. Khaneja, T. Reiss, C. Kehlet, T. Schulte-Herbrüggen, and S. J. Glaser, J. Magn. Reson. **172**, 296 (2005).

[45] G. Burkard, Phys. Rev. B **79**, 125317 (2009).

[46] P. Delsing, A. N. Cleland, M. J. A. Schuetz, J. Knörzer, G. Giedke, J. I. Cirac, K. Srinivasan, M. Wu, K. C. Balram, C. Bäuerle *et al.*, J. Phys. D: Appl. Phys. **52**, 353001 (2019).

[47] H.-T. Tan and W.-M. Zhang, Phys. Rev. A **83**, 032102 (2011).

[48] R. Dorner, S. R. Clark, L. Heaney, R. Fazio, J. Goold, and V. Vedral, Phys. Rev. Lett. **110**, 230601 (2013).

[49] P. Haikka, S. McEndoo, and S. Maniscalco, Phys. Rev. A **87**, 012127 (2013).

[50] D. Tamascelli, C. Benedetti, S. Olivares, and M. G. A. Paris, Phys. Rev. A **94**, 042129 (2016).

[51] M. Tukiainen, H. Lyyra, G. Sarbicki, and S. Maniscalco, Phys. Rev. A **95**, 052102 (2017).